

Journal of Mechanics

<http://journals.cambridge.org/JOM>

Additional services for *Journal of Mechanics*:

Email alerts: [Click here](#)

Subscriptions: [Click here](#)

Commercial reprints: [Click here](#)

Terms of use : [Click here](#)



Mixed Convection Flow of a Micropolar Fluid Past a Vertical Stretching Surface in a Thermally Stratified Porous Medium with Thermal Radiation

Mostafa A.A. Mahmoud and Shimaa E. Waheed

Journal of Mechanics / Volume 29 / Issue 03 / September 2013, pp 461 - 470
DOI: 10.1017/jmech.2013.22, Published online: 01 May 2013

Link to this article: http://journals.cambridge.org/abstract_S1727719113000221

How to cite this article:

Mostafa A.A. Mahmoud and Shimaa E. Waheed (2013). Mixed Convection Flow of a Micropolar Fluid Past a Vertical Stretching Surface in a Thermally Stratified Porous Medium with Thermal Radiation. Journal of Mechanics, 29, pp 461-470
doi:10.1017/jmech.2013.22

Request Permissions : [Click here](#)

MIXED CONVECTION FLOW OF A MICROPOLAR FLUID PAST A VERTICAL STRETCHING SURFACE IN A THERMALLY STRATIFIED POROUS MEDIUM WITH THERMAL RADIATION

Mostafa A.A. Mahmoud

*Department of Mathematics
Faculty of Science
Benha University, Egypt*

Shimaa E. Waheed *

*Department of Mathematics
Faculty of Science
Benha University, Benha; Taif University, Taif, KSA*

ABSTRACT

This paper is concerned with the effect of thermally stratification on the steady, two-dimensional mixed convection flow of a micropolar fluid past a vertical stretching permeable surface saturated in porous medium taking into account the effect of thermal radiation. The governing system of partial differential equations describing the problem are converted into a system of non-linear ordinary differential equations using similarity transformation. The resulting system of coupled nonlinear ordinary differential equations is solved numerically using the Chebyshev spectral method. The numerical results for the velocity, the micro-rotation and the temperature are displayed graphically showing the effects of various parameters like the buoyancy parameter, the radiation parameter, the stratification parameter, the permeability parameter and the suction/injection parameter. Moreover, the numerical values of the local skin-friction coefficient, the wall couple stress and the local Nusselt number for these parameters are also tabulated and discussed.

Keywords: Micropolar fluid, Mixed convection, Stretching plate, Thermally stratified porous medium, Thermal radiation.

1. INTRODUCTION

The study of non-Newtonian fluid flows have gained much attention by the researchers because of its applications in biology, physiology, technology and industry. In addition, the effects of heat transfer in non-Newtonian fluid saturated porous media also have great importance in engineering applications like the thermal design of industrial equipment dealing with molten plastics, polymeric liquids, or slurries. Several investigators have extended many of the available convective heat transfer in fluid saturated porous media problems to include the non-Newtonian effects. More discussion and applications of convective transport in porous media can be found in the book by Nield and Bejan [1], Ingham and Pop [2,3], Vafai [4,5], Pop and Ingham [6], Ingham *et al.* [7] and Bejan *et al.* [8]. There are several models for non-Newtonian fluids depending on the constitutive relationships between stress and rate of strain one of them is a micropolar fluid. The early studies of Eringen [9,10] have reported results on the theory of a micropolar fluids. Extensive reviews of this theory and its applications can be found in the articles by Ariman *et al.* [11,12] and the recent books by Lukaszewicz [13] and Eringen [14]. Mixed convection of a micropolar fluid over a moving surface have been studied by many authors [15-19] under

different situations. Recently, Gupta and Sharma [20] studied the thermal instability of a micropolar fluid through a porous medium that has a constant thickness. Raptis [21] studied the steady boundary layer flow of a micropolar fluid through a porous medium by using the generalized Darcys law.

In spite of the extensive research over the past few decades, there are still some fundamental problems that need to be understood. One of them is the convective transport in thermally stratified porous medium because of the broad range of engineering applications. They include heat rejection into the environment such as lakes, rivers and seas, thermal energy storage systems such as solar ponds, and heat transfer from thermal sources such as the condensers of power plants. Although this thermal stratification effect on heat transfer in porous medium is important, only limited number of references are available in the literature, only for certain special cases. An early study of natural convection heat transfer from a semi-infinite vertical plate immersed in a thermally stratified medium was first conducted by Cheesewright [22]. Chen and Eichhorn [23] used boundary-layer approach to study free convective heat transfer for a thermally-stratified regime. Vekatachala [24] also studied free convection in thermally-stratified fluids. Kulkarni *et al.* [25] studied the problem of natural convection flow over

* Corresponding author (shimaa_ezat@yahoo.com)

an isothermal vertical wall immersed in a thermally stratified medium and reported the similarity solutions. Angirasa and Srinivasan [26] have presented a numerical study of the natural convection flow on a vertical surface due to the combined effect of buoyancy forces caused by the heat and mass diffusion in a thermally stratified medium. Recently, Takhar *et al.* [27] studied numerically the free convection boundary layer flow over a continuously moving isothermal vertical surface in a thermally-stratified medium. The steady mixed convection boundary layer flow through a stable stratified medium adjacent to a vertical surface investigated by Ishak *et al.* [28]. Bejan [29] also studied the classical problem of steady free convection boundary layer flow past a vertical plate in a thermally stratified porous medium. Cheng and Lee [30] studied the flow and heat transfer characteristics of the free convection on a vertical plate with uniform and constant heat flux in a thermally stratified micropolar fluid.

In many engineering new areas such as fossil fuel combustion energy processes, solar power technology, astrophysical flows, and space vehicle re-entry occur at high temperatures, so knowledge of radiation heat transfer beside the convective heat transfer play a very important role and cannot be neglected. Also, the effect of thermal radiation on flow and heat transfer processes is of major importance in the design of many advanced energy conversion systems operating at high temperature. Thermal radiation within such systems occur because of the emission from the hot walls and working fluid. In view of this, Perdakis and Raptis [31] studied the heat of a micropolar fluid in the presence of radiation. The effects of radiation on the flow and heat transfer of a micropolar fluid past a continuously moving plate have been studied by many authors [32-34]. Recently, Raptis [35] has analyzed thermal radiation and free convection flow through a porous medium.

The objective of the present work is to investigate the two-dimensional mixed convection flow of a micropolar fluid over a stretching vertical permeable surface embedded in thermally stratified porous medium in the presence of radiation.

2. FORMULATION OF THE PROBLEM

Consider the steady, incompressible, two-dimensional laminar mixed convection boundary layer flow of a micropolar fluid over a stretching vertical flat plate of temperature $T_w(x)$, which is embedded in a thermally stratified porous medium of variable ambient temperature $T_\infty(x)$, where $T_w(x) > T_\infty(x)$. It is assumed that $T_w(x) = T_0 + bx$, $T_\infty(x) = T_0 + cx$ and the velocity of the stretching sheet $u_w(x) = ax$, where a , b and c are constants (with $a > 0$, $b > 0$, $c = dT_\infty / dx > 0$ is the stratification rate or the slope of the ambient temperature profile with vertical distance), T_0 is the ambient temperature at the leading edge of the plate, ($x = 0$) and x measures the distance from the leading edge along the surface of the plate.

The stationary Cartesian coordinate system has its origin located at the leading edge of the sheet with the positive x -axis extending along the sheet in the upwards direction, while the y -axis is measured normal to the surface of the sheet and is positive in the direction from the sheet to the fluid. We assume that all physical properties of the fluid are constants except the density in the buoyancy term. Under usual boundary layer and Boussinesq approximations, the governing boundary layer equations are given by the following equations:

$$u \frac{\partial u}{\partial x} + v \frac{\partial v}{\partial y} = 0, \quad (1)$$

$$u \frac{\partial u}{\partial x} + v \frac{\partial u}{\partial y} = \left(\frac{\mu + k}{\rho} \right) \frac{\partial^2 u}{\partial y^2} + \frac{k}{\rho} \frac{\partial N}{\partial y} - \frac{\mu}{\rho k_1} u + g\beta(T - T_\infty), \quad (2)$$

$$u \frac{\partial N}{\partial x} + v \frac{\partial N}{\partial y} = \frac{\gamma_0}{\rho j} \frac{\partial^2 N}{\partial y^2} - \frac{k}{\rho j} \left(2N + \frac{\partial u}{\partial y} \right), \quad (3)$$

$$u \frac{\partial T}{\partial x} + v \frac{\partial T}{\partial y} = \frac{\kappa}{\rho c_p} \frac{\partial^2 T}{\partial y^2} - \frac{1}{\rho c_p} \frac{\partial q_r}{\partial y}, \quad (4)$$

subject to the boundary conditions:

$$y = 0: \quad u = u_w(x) = ax, \quad v = v_w, \\ N = -m_0 \frac{\partial u}{\partial y}, \quad T = T_w(x) = T_0 + bx, \quad (5)$$

$$y \rightarrow \infty: \quad u \rightarrow 0, \quad N \rightarrow 0, \quad T \rightarrow T_\infty(x) = T_0 + cx,$$

where u and v are the velocity components in the x and y directions; respectively. T is the fluid temperature, N is the component of the micro-rotation vector normal to the xy -plane, k is the gyro-viscosity, μ is the dynamic viscosity, k_1 is the permeability, ρ is the density of the fluid, β is the thermal expansion coefficient, g is the gravitational acceleration acts in the downward direction, κ is the thermal conductivity, c_p is the specific heat at constant pressure, q_r is the radiation heat flux, γ_0 is the spin-gradient viscosity.

We follow the recent work of the authors [36,37] assuming that γ_0 is given by:

$$\gamma_0 = (\mu + k/2)j = \mu(1 + K/2)j. \quad (6)$$

This equation gives a relation between the coefficient of viscosity and microinertia, where $K = k/\mu (> 0)$ is the material parameter, $j = v/c$, \sqrt{j} is the reference length and $m_0 (0 \leq m_0 \leq 1)$ is the boundary parameter. When the boundary parameter $m_0 = 0$, we obtain $N = 0$ which is the no-spin condition *i.e.* the microelements in a concentrated particle flow close to the wall are not able to rotate (as stipulated by Jena and Mathur [38]). The case $m_0 = 1/2$, represents the weak concentration of microelements. The case corresponding to $m_0 = 1$ is used for the modelling of turbulent boundary layer flow (see Peddison and Mc Nitt [39]).

Using Rosseland approximation we have:

$$q_r = -(4\sigma^*/3k^*) \frac{\partial T^4}{\partial y}, \quad (7)$$

where σ^* is the Stefan Boltzmann constant and k^* is the mean absorption coefficient.

Assuming that the temperature differences within the flow are sufficiently small such that T^4 may be expressed as a linear function of temperature [40]:

$$T^4 \cong 4T_\infty^3 T - 3T_\infty^4, \quad (8)$$

where the higher-order terms of the expansion are neglected.

We introduce the following dimensionless variables:

$$\eta = \left[\frac{a}{v} \right]^{1/2} y, \quad N = ax \left[\frac{a}{v} \right]^{1/2} h(\eta),$$

$$u = ax f'(\eta), \quad v = -(av)^{1/2} f(\eta), \quad (9)$$

$$\theta(\eta) = \frac{T - T_\infty}{T_w - T_0}, \quad T_w - T_0 > 0.$$

Through Eq. (9), the continuity Eq. (1) is automatically satisfied and Eqs. (2) ~ (5)

are given by:

$$(1+K)f''' + ff'' - f'^2 + Kh' - D_a^{-1}f' + \lambda\theta = 0, \quad (10)$$

$$\left(1 + \frac{K}{2}\right)h'' + fh' - f'h - K(2h + f'') = 0, \quad (11)$$

$$(1+R)\theta'' + \text{Pr}(f\theta' - f'\theta - Sf') = 0, \quad (12)$$

The transformed boundary conditions are then given by:

$$\eta = 0: f = f_w, f' = 1, h = -m_0 f'', \theta = 1 - S, \quad (13)$$

$$\eta \rightarrow \infty: f' \rightarrow 0, h \rightarrow 0, \theta \rightarrow 0,$$

where primes denote differentiation with respect to η , $\lambda = g\beta b/a^2 (\geq 0)$ is the buoyancy parameter, $f_w = -v_w/(av)^{1/2}$ is the suction (> 0) or the injection parameter (< 0), $D_a^{-1} = v/ak_1$ is the permeability parameter, $\text{Pr} = \mu c_p/\kappa$ is the Prandtl number, $R = (16\sigma^* T_\infty^3)/(3k^* \kappa)$ is the radiation parameter and $S = c/d$ is the stratification parameter. We notice that $S > 0$ implies a stably stratified environment, while $S = 0$ corresponds to an unstratified environment.

The physical quantities of interest are the local skin-friction coefficient C_{f_x} , the dimensionless wall couple stress M_x and the local Nusselt number N_{u_x} , which are respectively; defined as:

$$C_{f_x} = \frac{2\tau_w}{\rho(ax)^2},$$

$$M_x = \frac{m_w}{\rho a^2 x^3}, \quad (14)$$

$$Nu_x = \frac{xq_w}{\kappa(T_w - T_0)},$$

where the local wall shear stress τ_w , the wall couple stress m_w and the heat transfer from the plate q_w are defined by:

$$\tau_w = - \left[(\mu + k) \frac{\partial u}{\partial y} + kN \right]_{y=0},$$

$$m_w = \gamma_0 \left[\frac{\partial N}{\partial y} \right]_{y=0}, \quad (15)$$

$$q_w = - \left[\kappa \frac{\partial T}{\partial y} \right]_{y=0}.$$

Using the similarity variables (9), we get:

$$\frac{1}{2} C_{f_x} \text{Re}_x^{1/2} = -(1 + K(1 - m_0)) f''(0),$$

$$M_x \text{Re}_x = \left(1 + \frac{K}{2}\right) h'(0), \quad (16)$$

$$N_{u_x} \text{Re}_x^{-1/2} = -\theta'(0),$$

where $\text{Re}_x = \left(\frac{ax^2}{v}\right)$ is the local Reynolds number.

3. METHOD OF SOLUTION

The domain of the governing boundary layer Eqs. (10) ~ (13) is the unbounded region $[0, \infty)$. However, for all practical reasons, this could be replaced by the interval $0 \leq \eta \leq \eta_\infty$, where η_∞ is one end of the user specified computational domain.

Using the algebraic mapping:

$$\chi = 2 \frac{\eta}{\eta_\infty} - 1. \quad (17)$$

The unbounded region $[0, \infty)$ is mapped into the finite domain $[-1, 1]$, and the problem expressed by Eqs. (10) ~ (13) is transformed into:

$$(1+K)f'''(\chi) + \left(\frac{\eta_\infty}{2}\right) (f(\chi)f''(\chi) - f'^2(\chi))$$

$$+ \left(\frac{\eta_\infty}{2}\right)^2 (Kh'(\chi) - D_a^{-1}f'(\chi)) + \left(\frac{\eta_\infty}{2}\right)^3 \lambda\theta(\chi) = 0, \quad (18)$$

$$\left(1 + \frac{K}{2}\right)h''(\chi) + \left(\frac{\eta_\infty}{2}\right) (f(\chi)h'(\chi) - f'(\chi)h(\chi))$$

$$- K \left(2 \left(\frac{\eta_\infty}{2}\right)^2 h(\chi) + f''(\chi)\right) = 0, \quad (19)$$

$$(1+R)\theta''(\chi) + \left(\frac{\eta_\infty}{2}\right) \Pr(f(\chi)\theta'(\chi) - f'(\chi)\theta(\chi) - Sf'(\chi)) = 0, \quad (20)$$

The transformed boundary conditions are then given by:

$$f(-1) = f_w, \quad f'(-1) = \left(\frac{\eta_\infty}{2}\right), \quad f'(1) = 0, \\ h(-1) = -m_0 \left(\frac{2}{\eta_\infty}\right)^2 f''(-1), \quad h(1) = 0, \quad (21)$$

$$\theta(-1) = 1 - S, \quad \theta(1) = 0,$$

where now differentiation in Eqs. (17) ~ (20) will be with respect to the new variable χ .

Our technique is accomplished by starting with a Chebyshev approximation for the highest order derivatives, f''' , h'' and θ'' and generating approximations to the lower order derivatives f'' , f' , f , h' , h , θ' and θ as follows:

Setting $f''' = \phi(\chi)$, $h'' = \psi(\chi)$ and $\theta'' = \zeta(\chi)$, then by integration we obtain:

$$f''(\chi) = \int_{-1}^{\chi} \phi(\chi) d\chi + C_1^f, \quad (21)$$

$$f'(\chi) = \int_{-1}^{\chi} \int_{-1}^{\chi} \phi(\chi) d\chi d\chi + C_1^f(\chi+1) + C_2^f, \quad (22)$$

$$f(\chi) = \int_{-1}^{\chi} \int_{-1}^{\chi} \int_{-1}^{\chi} \phi(\chi) d\chi d\chi d\chi + C_1^f \frac{(\chi+1)^2}{2} + C_2^f(\chi+1) + C_3^f, \quad (23)$$

$$h'(\chi) = \int_{-1}^{\chi} \psi(\chi) d\chi + C_1^h, \quad (24)$$

$$h(\chi) = \int_{-1}^{\chi} \int_{-1}^{\chi} \psi(\chi) d\chi d\chi + C_1^h(\chi+1) + C_2^h. \quad (25)$$

$$\theta'(\chi) = \int_{-1}^{\chi} \zeta(\chi) d\chi + C_1^\theta, \quad (26)$$

$$\theta(\chi) = \int_{-1}^{\chi} \int_{-1}^{\chi} \zeta(\chi) d\chi d\chi + C_1^\theta(\chi+1) + C_2^\theta. \quad (27)$$

From the boundary condition (20), we obtain:

$$C_1^f = -\frac{1}{2} \left(\frac{\eta_\infty}{2}\right) - \frac{1}{2} \int_{-1}^1 \int_{-1}^{\chi} \phi(\chi) d\chi d\chi,$$

$$C_2^f = \left(\frac{\eta_\infty}{2}\right),$$

$$C_3^f = f_w,$$

$$C_1^h = -\frac{1}{2} \int_{-1}^1 \int_{-1}^{\chi} \psi(\chi) d\chi d\chi - \frac{1}{2} C_2^h,$$

$$C_2^h = \frac{m_0}{2} \left(\frac{2}{\eta_\infty}\right) + \frac{m_0}{2} \left(\frac{2}{\eta_\infty}\right)^2 \int_{-1}^1 \int_{-1}^{\chi} \psi(\chi) d\chi d\chi,$$

$$C_1^\theta = -\frac{1}{2} \int_{-1}^1 \int_{-1}^{\chi} \zeta(\chi) d\chi d\chi - \frac{1}{2} C_2^\theta,$$

$$C_2^\theta = 1 - S.$$

Therefore, we can give approximations to Eqs. (21) ~ (27) as follows:

$$f_i(\chi) = \sum_{j=0}^n l_{ij}^f \phi_j + d_i^f, \quad f'_i(\chi) = \sum_{j=0}^n l_{ij}^{f'} \phi_j + d_i^{f'}, \\ f''_i(\chi) = \sum_{j=0}^n l_{ij}^{f''} \phi_j + d_i^{f''}, \quad (28)$$

$$h_i(\chi) = \sum_{j=0}^n l_{ij}^h \psi_j + \sum_{j=0}^n l_{ij}^h \phi_j + d_i^h, \\ h'_i(\chi) = \sum_{j=0}^n l_{ij}^{h'} \psi_j + \sum_{j=0}^n l_{ij}^{h'} \phi_j + d_i^{h'}, \quad (29)$$

$$\theta_i(\chi) = \sum_{j=0}^n l_{ij}^\theta \zeta_j + d_i^\theta, \quad \theta'_i(\chi) = \sum_{j=0}^n l_{ij}^{\theta'} \zeta_j + d_i^{\theta'}, \quad (30)$$

for all $i = 0(1)n$, where

$$l_{ij}^\theta = b_{ij}^2 - \frac{(\chi_i+1)}{2} b_{nj}^2, \quad d_i^\theta = (1-S) \left(1 - \frac{(\chi_i+1)}{2}\right),$$

$$l_{ij}^{\theta'} = b_{ij} - \frac{1}{2} b_{nj}^2, \quad d_i^{\theta'} = -\frac{(1-S)}{2},$$

$$l_{ij}^h = \frac{m_0}{2} \left(\frac{2}{\eta_\infty}\right)^2 \left(1 - \frac{(\chi_i+1)}{2}\right) b_{nj}^2,$$

$$d_i^h = \frac{m_0}{2} \left(\frac{2}{\eta_\infty}\right) \left(1 - \frac{(\chi_i+1)}{2}\right),$$

$$l_{ij}^{h'} = -\frac{m_0}{4} \left(\frac{2}{\eta_\infty}\right)^2 b_{nj}^2, \quad d_i^{h'} = -\frac{m_0}{4} \left(\frac{2}{\eta_\infty}\right),$$

$$l_{ij}^f = b_{ij}^3 - \frac{(\chi_i+1)^2}{4} b_{nj}^2,$$

$$d_i^f = \left(\frac{\eta_\infty}{2}\right) \left((\chi_i+1) - \frac{(\chi_i+1)^2}{4} + f_w \right),$$

$$l_{ij}^{f'} = b_{ij}^2 - \frac{(\chi_i+1)}{2} b_{nj}^2, \quad d_i^{f'} = \left(\frac{\eta_\infty}{2}\right) \left(1 - \frac{(\chi_i+1)}{2}\right),$$

$$l_{ij}^{f''} = b_{ij} - \frac{1}{2} b_{nj}^2, \quad d_i^{f''} = -\frac{1}{2} \left(\frac{\eta_\infty}{2}\right),$$

where

$$b_{ij}^2 = (\chi_i - \chi_j) b_{ij}, \quad i = 0(1)n,$$

and b_{ij} are the elements of the matrix B , as given in Ref. [41,42].

By using Eqs. (28) ~ (30), one can transform Eqs. (17) ~ (19) to the following system of nonlinear equations in the highest derivatives:

$$(1+K)\phi_i + \left(\frac{\eta_\infty}{2}\right) \left[\left(\sum_{j=0}^n l_{ij}^f \phi_j + d_i^f \right) \left(\sum_{j=0}^n l_{ij}^{f_2} \phi_j + d_i^{f_2} \right) - \left(\sum_{j=0}^n l_{ij}^{f_1} \phi_j + d_i^{f_1} \right)^2 \right] + \left(\frac{\eta_\infty}{2}\right)^2 \left(K \left(\sum_{j=0}^n l_{ij}^{\theta_1} \psi_j + \sum_{j=0}^n l_{ij}^h \phi_j + d_i^h \right) - D_a^{-1} \left(\sum_{j=0}^n l_{ij}^{f_1} \phi_j + d_i^{f_1} \right) \right) + \left(\frac{\eta_\infty}{2}\right)^3 \lambda \left(\sum_{j=0}^n l_{ij}^{\theta} \zeta_j + d_i^{\theta} \right) = 0, \quad (31)$$

$$\left(1 + \frac{K}{2}\right) \psi_i + \left(\frac{\eta_\infty}{2}\right) \left[\left(\sum_{j=0}^n l_{ij}^f \phi_j + d_i^f \right) \left(\sum_{j=0}^n l_{ij}^{\theta_1} \psi_j + \sum_{j=0}^n l_{ij}^h \phi_j + d_i^h \right) - \left(\sum_{j=0}^n l_{ij}^{f_1} \phi_j + d_i^{f_1} \right) \left(\sum_{j=0}^n l_{ij}^{\theta} \psi_j + \sum_{j=0}^n l_{ij}^h \phi_j + d_i^h \right) \right] - K \left(2 \left(\frac{\eta_\infty}{2}\right)^2 \left[\left(\sum_{j=0}^n l_{ij}^{\theta} \psi_j + \sum_{j=0}^n l_{ij}^h \phi_j + d_i^h \right) + \left(\sum_{j=0}^n l_{ij}^{f_2} \phi_j + d_i^{f_2} \right) \right] \right) = 0, \quad (32)$$

$$(1+R)\zeta_i + \left(\frac{\eta_\infty}{2}\right) \text{Pr} \left[\left(\sum_{j=0}^n l_{ij}^f \phi_j + d_i^f \right) \left(\sum_{j=0}^n l_{ij}^{\theta_1} \zeta_j + d_i^{\theta_1} \right) - \left(\sum_{j=0}^n l_{ij}^{f_1} \phi_j + d_i^{f_1} \right) \left(\sum_{j=0}^n l_{ij}^{\theta} \zeta_j + d_i^{\theta} \right) - S \left(\sum_{j=0}^n l_{ij}^f \phi_j + d_i^f \right) \right] = 0. \quad (33)$$

This system is solved using Newton's iteration. The computer program of the numerical method was executed in MATHEMATICA 4 running on PC.

4. RESULTS AND DISCUSSION

To verify the proper treatment of the problem, our numerical results have been compared for $f''(0)$ and $-\theta'(0)$ taking $K = 0$, $S = 0$, $f_w = 0$, $\text{Pr} = 1$ and $R = 0$ in Eqs. (10) and (12) with those obtained by Ishak *et al.* [43] (with $\text{Pr} = 1$, $\lambda = 1$, $m = 1$, $n = 1$ and we consider $D_a^{-1} = M$) and Ali *et al.* [44] (with $m = 0$, $\lambda = 1$ and $\text{Pr} = 1$) for various values of D_a^{-1} . The results of this comparison show a good agreement as seen in Table 1.

We have considered in some detail the influence of the various parameters such as the buoyancy parameter, the radiation parameter, the stratification parameter, the permeability parameter and the suction/injection parameter on the velocity, the micro-rotation and the temperature profiles which are shown in Figs. 1 ~ 10. The samples of the velocity and micro-rotation profiles for the different values of the buoyancy parameter λ when the other parameters fixed are presented in Fig. 1. It is seen from this that the dimensionless velocity f' increases with the increase of λ for $S = 0.1$ while the opposite is true for $S = 0.9$. The micro-rotation profiles h increase as λ increases near the surface and the inverse is true away from the surface with $S = 0.1$ and $S = 0.9$. Fig. 2 shows the effect of λ on temperature profiles θ . In the case of $S = 0.1$ the temperature decreases as the buoyancy parameter λ increases. The opposite is true in the case of $S = 0.9$. This is due to the fact that the effect of the stratification on the mean field is the formation of a region with a temperature deficit (*i.e.* a negative dimensionless temperature) in the outer part of the boundary layer. This phenomenon was first shown theoretically by Prandtl [45] for an infinite wall and later on by Jaluria and Himasekhar [46] for semi-infinite walls, utilizing finite difference techniques.

Figure 3 display the influence of R on f' and h . It is

obvious that for both cases of $S = 0.1$ and $S = 0.9$, f' increases as R increases, while h decreases with the increase of R near the surface and the opposite is true away from it. An increase of thermal radiation added more heat within the fluid which interacts with the buoyancy force to induce the flow in the boundary layer causing velocity of the fluid there to increase. Figure 4 illustrates the temperature profiles with various values of R for a given S ($S = 0.1$ or $S = 0.9$). It is observed that the temperature increases with an increase of R . The increase of radiation parameter R implies the release of heat energy from the flow region by means of radiation; this can also be explained by the fact that the effect of radiation is to increase the rate of energy transport to the fluid and accordingly increase the fluid temperature.

Table 1 Comparison of $f''(0)$ and $-\theta'(0)$ for various values of D_a^{-1} with $R = 0$, $K = 0$, $S = 0$, $\text{Pr} = 1$ and $\lambda = 1$

D_a^{-1}	Ishak <i>et al.</i> [43]		Ali <i>et al.</i> [44]		Present results	
	$f''(0)$	$-\theta'(0)$	$f''(0)$	$-\theta'(0)$	$f''(0)$	$-\theta'(0)$
0	-0.5607	1.0873	-0.5607	1.0873	-0.5607	1.0873
0.01	-0.5658	1.0863	-0.5658	1.0863	-0.5658	1.0863
0.04	-0.5810	1.0833	-0.5810	1.0833	-0.5810	1.0833
0.25	-0.6830	1.0630	-0.6830	1.0630	-0.6830	1.0630
1	-1.0000	1.0000	-1.0000	1.0000	-1.0000	1.0000
4	-1.8968	0.8311	-1.8968	0.8311	-1.8968	0.8311
25	-4.9155	0.4702	-4.9155	0.4702	-4.9155	0.4702

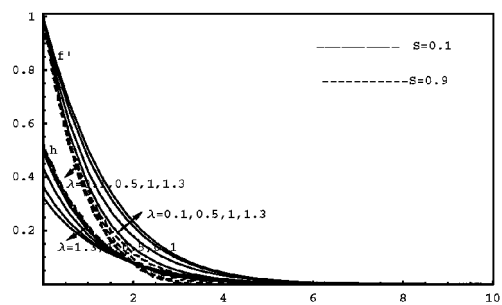


Fig. 1 Velocity and microrotation profiles for various values of λ with $f_w = 0.2$, $D_a^{-1} = 0.5$, $R = 0.3$, $K = 1.2$ and $\text{Pr} = 0.72$

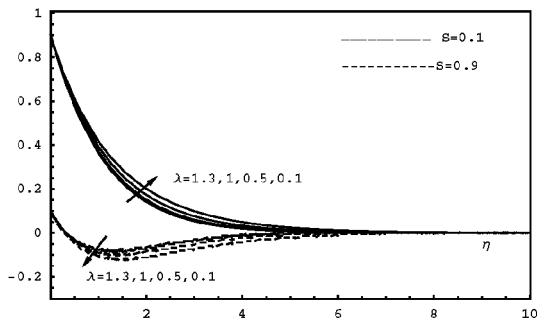


Fig. 2 Temperature profiles for various values of λ with $f_w = 0.2$, $D_a^{-1} = 0.5$, $R = 0.3$, $K = 1.2$ and $Pr = 0.72$

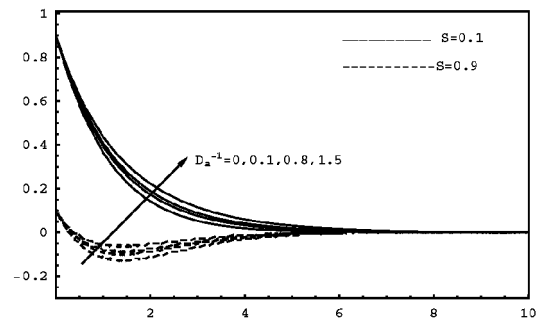


Fig. 6 Temperature profiles for various values of D_a^{-1} with $f_w = 0.2$, $R = 0.3$, $\lambda = 0.5$, $K = 1.2$ and $Pr = 0.72$

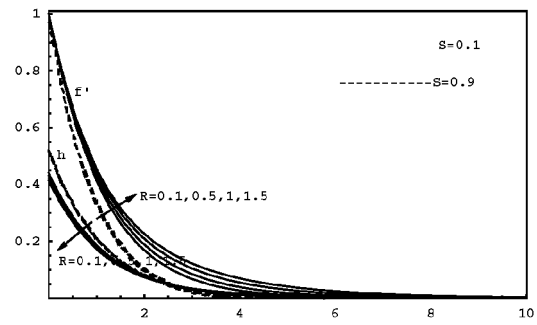


Fig. 3 Velocity and microrotation profiles for various values of R with $f_w = 0.2$, $D_a^{-1} = 0.5$, $\lambda = 0.5$, $K = 1.2$ and $Pr = 0.72$

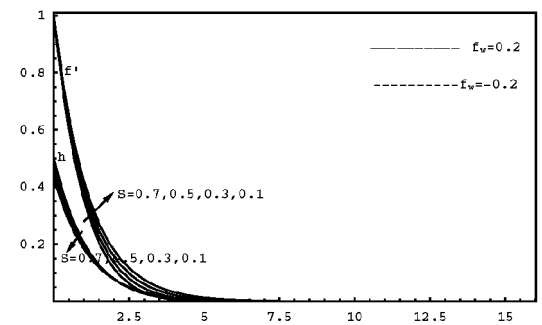


Fig. 7 Velocity and microrotation profiles for various values of S with $\lambda = 0.5$, $D_a^{-1} = 0.5$, $R = 0.3$, $K = 1.2$ and $Pr = 0.72$

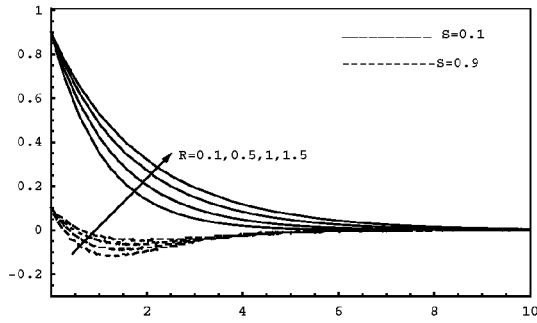


Fig. 4 Temperature profiles for various values of R with $f_w = 0.2$, $D_a^{-1} = 0.5$, $\lambda = 0.5$, $K = 1.2$ and $Pr = 0.72$

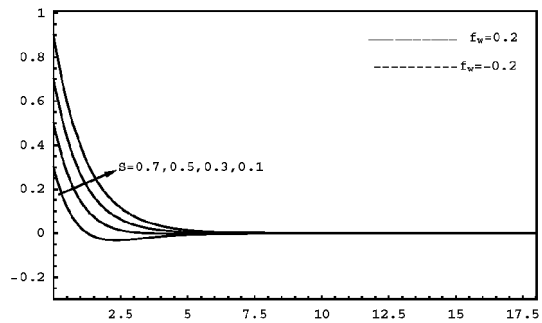


Fig. 8 Temperature profiles for various values of S with $\lambda = 0.5$, $D_a^{-1} = 0.5$, $R = 0.3$, $K = 1.2$ and $Pr = 0.72$

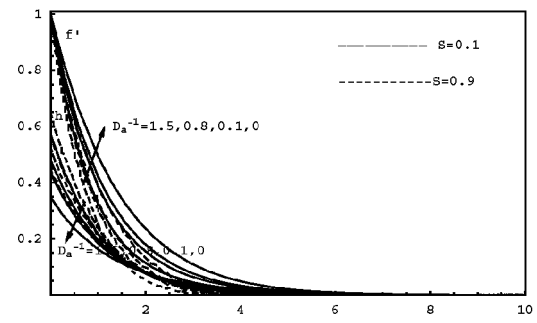


Fig. 5 Velocity and microrotation profiles for various values of D_a^{-1} with $f_w = 0.2$, $R = 0.3$, $\lambda = 0.5$, $K = 1.2$ and $Pr = 0.72$

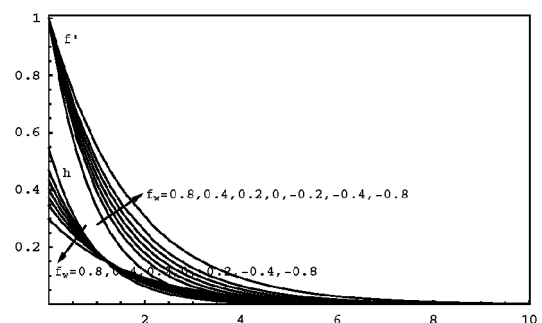


Fig. 9 Velocity and microrotation profiles for various values of f_w with $S = 0.1$, $D_a^{-1} = 0.5$, $R = 0.3$, $\lambda = 0.5$, $K = 1.2$ and $Pr = 0.72$

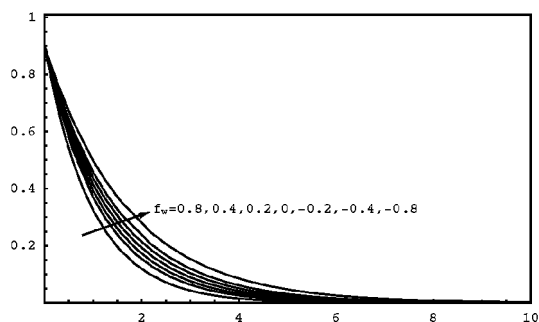


Fig. 10 Temperature profiles for various values of f_w with $S = 0.1$, $D_a^{-1} = 0.5$, $R = 0.3$, $\lambda = 0.5$, $K = 1.2$ and $Pr = 0.72$

Figure 5 presents the effect of the permeability parameter D_a^{-1} on f' and h . We notice that for $S = 0.1$ and $S = 0.9$, f' decreases with the increase of D_a^{-1} , but h increases as D_a^{-1} increases, the opposite is true at a large distance from the plate which means that porous medium acts as an hindrance in the rotary motions of the micro-elements. Also, it should be noticed that large values of D_a correspond to high porosity of the porous medium, and the limit $D_a \rightarrow \infty$ corresponds to the case of no porous medium is present. Obviously a high porosity of the porous medium exerts less resistance to the flow. The presence of porous medium causes higher retardation to the fluid, which reduces the velocity. Figure 6 illustrates the effects of D_a^{-1} on the temperature profiles θ . It is observed that θ increases with the increase of D_a^{-1} for both cases of $S = 0.1$ and $S = 0.9$.

Figure 7 shows the variation of $f'(\eta)$ and $h(\eta)$ with η for various values of the stratification parameter S . It is seen that f' decreases with the increase of S , while h increases with the increase of S near the surface and h decreases at larger distance from the surface. Figure 8 shows the effect of S on θ . Where one sees that the temperature profiles decrease as S increases. Figure 8 also shows the curve for $S = 0.9$, to emphasize the presence of negative θ , or local temperature undershoot, which apparently arises with extreme stratification. This effect was also observed in the calculations of Cheesewright [22], who suggested that such a temperature undershoot constitutes an unstable situation and may, therefore, impart heightened instability to the boundary region.

The effects of suction (injection) parameter f_w on the velocity micro-rotation profiles are shown in Fig. 9. It is evident from this figure that the velocity increases as the transpiration rate at the plate goes from suction ($f_w = 0.8$) to injection ($f_w = -0.8$). Also, it is observed that as f_w increases from suction ($f_w = 0.8$) to injection ($f_w = -0.8$) the micro-rotation decreases near the surface and the reverse is true at larger distance from the surface. The temperature profiles with variation of f_w has been shown in Fig. 10. It is observed that as f_w increases from suction to injection, the effect is to higher the temperature levels in the thermal boundary layer.

The local skin-friction coefficient in the term of $-f''(0)$, the wall couple stress in the term of $h'(0)$ and the local Nusselt number in the term of $-\theta'(0)$ for various values of λ , R , S , f_w and D_a^{-1} are illustrated in Table 2. From this Table one observes that for $S = 0.1$, λ has the effect of decreasing the local skin-friction coefficient. The local Nusselt number and the wall couple stress increase with increasing λ . The opposite is true for $S = 0.9$. Moreover, increasing R reduce the local skin-friction coefficient and the local Nusselt number, while the wall couple stress increases as R increases for both cases of $S = 0.1$ and $S = 0.9$. The local skin friction coefficient increases with increasing S , but the local Nusselt number and the wall couple stress decrease with increasing S . The local skin friction coefficient and the local Nusselt number decrease in the presence of injection but they increase in the presence of suction at the surface. The inverse is true for the wall couple stress. Finally, the local skin friction coefficient increases with increasing D_a^{-1} , but the local Nusselt number and the wall couple stress decrease with increasing D_a^{-1} for both cases of $S = 0.1$ and $S = 0.9$.

5. CONCLUSIONS

The problem of steady, two-dimensional mixed convection flow of a micropolar fluid over stretching permeable vertical surface with radiation taking into account the presence thermally stratification has been investigated. Using similarity transformations, the governing equations have been transformed into a system of coupled non-linear ordinary differential equations which is solved numerically by using the Chebyshev spectral method. The effects of various parameters λ , R , S , f_w , D_a^{-1} and Pr on the flow and heat characteristics were examined. It was found that the local skin-friction coefficient decreases as the radiation parameter increases, while it increases as the permeability parameter increases for both cases of $S = 0.1$ and $S = 0.9$. It is also found that the wall couple stress increases as the radiation parameter increases, while it decreases as the permeability parameter increases for both cases of $S = 0.1$ and $S = 0.9$. The local Nusselt number decreases as the radiation parameter and the permeability parameter increase for a given S ($S = 0.1$ and $S = 0.9$). For $S = 0.1$, the buoyancy parameter has the effect of decreasing the local skin-friction coefficient, while the local Nusselt number and the wall couple stress increase with increasing the buoyancy parameter. The opposite is true for $S = 0.9$. The local skin friction coefficient increases with increasing the stratification parameter, but the local Nusselt number and the wall couple stress decrease with increasing the stratification parameter. Also, it was found that the local skin friction coefficient and the local Nusselt number decrease in the presence of injection but they increase in the presence of suction at the surface, while the inverse is true for the wall couple stress.

ACKNOWLEDGMENTS

The authors would like to thank the reviewers for their valuable comments, which led to the improvement of the work.

Table 2 Values of $-f''(0)$, $h'(0)$ and $-\theta'(0)$ with $m_0 = 0.5$, $K = 1.2$ and $Pr = 0.72$

λ	R	S	f_w	D_a^{-1}	$-f''(0)$	$h'(0)$	$-\theta'(0)$
0.1	0.3	0.1	0.2	0.5	0.991905	-0.439398	0.719753
0.5	0.3	0.1	0.2	0.5	0.869536	-0.374131	0.751623
1	0.3	0.1	0.2	0.5	0.729524	-0.294924	0.780288
1.3	0.3	0.1	0.2	0.5	0.649904	-0.248254	0.794439
0.1	0.3	0.9	0.2	0.5	1.030220	-0.457190	0.422879
0.5	0.3	0.9	0.2	0.5	1.044630	-0.459928	0.404184
1	0.3	0.9	0.2	0.5	1.055850	-0.461664	0.390889
1.3	0.3	0.9	0.2	0.5	1.060700	-0.462194	0.385200
0.5	0.1	0.1	0.2	0.5	0.880242	-0.377917	0.837098
0.5	0.5	0.1	0.2	0.5	0.860292	-0.371005	0.685503
0.5	1	0.1	0.2	0.5	0.841804	-0.365113	0.570177
0.5	1.5	0.1	0.2	0.5	0.827827	-0.360941	0.494867
0.5	0.1	0.9	0.2	0.5	1.048720	-0.461750	0.462194
0.5	0.5	0.9	0.2	0.5	1.041140	-0.458447	0.360068
0.5	1	0.9	0.2	0.5	1.034260	-0.455719	0.284974
0.5	1.5	0.9	0.2	0.5	1.029140	-0.453845	0.237455
0.5	0.3	0.1	0.2	0.5	0.869523	-0.374120	0.751611
0.5	0.3	0.3	0.2	0.5	0.913862	-0.396018	0.668458
0.5	0.3	0.5	0.2	0.5	0.957815	-0.417607	0.582814
0.5	0.3	0.7	0.2	0.5	1.001380	-0.438891	0.494715
0.5	0.3	0.1	0.8	0.5	1.089490	-0.590173	0.923716
0.5	0.3	0.1	0.4	0.5	0.938229	-0.436384	0.805552
0.5	0.3	0.1	0.2	0.5	0.869536	-0.374131	0.751623
0.5	0.3	0.1	0.0	0.5	0.805608	-0.320468	0.701193
0.5	0.3	0.1	-0.2	0.5	0.746449	-0.274491	0.654245
0.5	0.3	0.1	-0.4	0.5	0.691981	-0.235304	0.610712
0.5	0.3	0.1	-0.8	0.5	0.596472	-0.173905	0.533417
0.5	0.3	0.1	0.2	0.0	0.695909	-0.278853	0.790437
0.5	0.3	0.1	0.2	0.1	0.869536	-0.374131	0.751623
0.5	0.3	0.1	0.2	0.8	0.960326	-0.424739	0.731521
0.5	0.3	0.1	0.2	1.5	1.145730	-0.529651	0.691322
0.5	0.3	0.9	0.2	0.0	0.892742	-0.375414	0.438434
0.5	0.3	0.9	0.2	0.1	1.044630	-0.459928	0.404184
0.5	0.3	0.9	0.2	0.8	1.125510	-0.505617	0.387436
0.5	0.3	0.9	0.2	1.5	1.293260	-0.601750	0.355714

NOMENCLATURES

c_p	specific heat at constant pressure
C_x	local skin-friction coefficient
D_a^{-1}	permeability parameter
f	dimensionless velocity
f_w	dimensionless suction or injection velocity
g	gravitational acceleration acts in the downward direction
h	dimensionless micro-rotation
j	micro-inertia
k	gyro-viscosity
k_1	permeability
K	material parameter
k^*	mean absorption coefficient
m_0	boundary parameter
M_x	dimensionless wall couple stress
m_w	wall couple stress
N	dimensional component of micro-rotation vector normal to the xy -plane

N_{u_x}	local Nusselt number
Pr	Prandtl number
q_r	radiative heat flux
q_w	heat transfer from the plate
R	radiation parameter
Re_x	local Reynolds number
S	stratification parameter
T	fluid temperature
T_∞	temperature at the free surface
T_w	surface temperature of the plate
T_0	ambient temperature at leading edge of the plate
u, v	dimensional components of velocities along and perpendicular to the plate, respectively
u_w	surface velocity
v_w	dimensional suction or injection velocity
x, y	dimensional distances along and perpendicular to the plate, respectively

Greek symbols

η	dimensionless distance normal to the plate
γ_0	spin-gradient viscosity
σ^*	Stefan Boltzmann constant
κ	thermal conductivity
μ	dynamic viscosity
ρ	fluid density
τ_w	wall shear stress
β	thermal expansion coefficient
λ	buoyancy parameter
θ	dimensionless temperature

Subscripts

w	condition at the solid surface
0	ambient condition

Superscripts

$/$	differentiation with respect to η
-----	--

REFERENCES

1. Nield, D. A. and Bejan, A., *Convection in Porous Media*, 3rd Edition, Springer, New York (2006).
2. Ingham, D. B. and Pop, I. Des., *Transport Phenomena in Porous Media*, vol. II 2002, Pergamon, Oxford (1998).
3. Ingham, D. B. and Pop, I. Des., *Transport Phenomena in Porous Media*, I, III, Elsevier, Oxford (2005).
4. Vafai, K. Ed., *Handbook of Porous Media*, Marcel Dekker, New York (2000).
5. Vafai, K. Ed., *Handbook of Porous Media*, 2nd Edition, Taylor & Francis, New York (2005).
6. Pop I. and Ingham D. B., *Convective Heat Transfer: Mathematical and Computational Modelling of Viscous Fluids and Porous Media*, Pergamon Pr., Oxford (2001).
7. Ingham, D. B., Bejan, A., Mamut, E. and Pop, I. Eds., *Emerging Technologies and Techniques in*

- Porous Media*, Kluwer Academic Publishers, Dordrecht, The Netherlands (2004).
8. Bejan, A., Dincer, I., Lorente, S., Miguel, A.F. and Reis, A.H., *Porous and Complex Flow Structures in Modern Technologies*, Springer-Verlag, New York (2004).
 9. Eringen, A. C., "Theory of Micropolar Fluids," *Journal of Mathematics and Mechanics*, **16**, pp. 1–18 (1966).
 10. Eringen, A. C., "Theory of Thermomicropolar Fluids," *Journal of Mathematical Applications*, **38**, pp. 480–495 (1972).
 11. Armin, T., Turk, M. A. and Sylvester, N. D., "Microcontinuum Fluid Mechanics a Review," *International Journal of Engineering Science*, **11**, pp. 905–915 (1973).
 12. Armin, T., Turk, M. A. and Sylvester, N. D., "Application of Microcontinuum Fluid Mechanics," *International Journal of Engineering Science*, **12**, pp. 273–279 (1974).
 13. Lukaszewicz, G., *Micropolar Fluids: Theory and Application*, Birkhäuser, Basel (1999).
 14. Eringen, A. C., *Microcontinuum Field Theories, II: Fluent Media*, Springer, New York (2001).
 15. Bhargava, R., Kumar, L. and Takhar, H. S., "Mixed Convection from a Continuous Surface in a Parallel Moving Stream of a Micropolar Fluid," *Heat and Mass Transfer*, **39**, pp. 407–413 (2003).
 16. Rahman, M. M. and Sattar, M. A., "Transient Convective Flow of Micropolar Fluid Past a Continuously Moving Vertical Porous Plate in the Presence of Radiation," *International Journal of Applied Mechanics and Engineering*, **12**, pp. 497–513 (2007).
 17. Rahman, M. M. and Sattar, M. A., "Magnetohydrodynamic Convective Flow of a Micropolar Fluid Past a Continuously Moving Vertical Porous Plate in the Presence of Heat Generation/Absorption," *Journal of Heat Transfer*, ASME, **128**, pp. 142–152 (2006).
 18. Ishak, A., Nazar, R. and Pop, I., "Mixed Convection Stagnation Point Flow of a Micropolar Fluid Towards a Stretching Sheet," *Meccanica*, **43**, pp. 411–418 (2008).
 19. Hayat, T., Abbas, Z. and Javed, T., "Mixed Convection Flow of a Micropolar Fluid over a Non-Linearly Stretching Sheet," *Physics Letters A*, **372**, pp. 637–647 (2008).
 20. Gupta, U. and Sharma, R. S., "Thermal Convection in Micropolar Fluids in Porous Medium," *International Journal of Engineering Science*, **33**, pp. 1887–1892 (1995).
 21. Raptis, A., "Boundary Layer Flow of a Micropolar Fluid Through a Porous Medium," *Journal of Porous Media*, **3**, pp. 95–96 (2000).
 22. Cheesewright, R., "Natural Convection from a Plane Vertical Surface in Non-Isothermal Surroundings," *International Journal Heat and Mass Transfer*, **10**, pp. 1847–1859 (1967).
 23. Chen, C. C. and Eichhorn, R., "Natural Convection from a Vertical Surface to a Thermally Stratified Fluid," *Journal of Heat Transfer*, ASME, **98**, pp. 446–451 (1976).
 24. Venkatachala, B. J. and Nath, G., "Non-Similar Laminar Natural Convection in a Thermally Stratified Fluid," *International Journal Heat and Mass Transfer*, **24**, pp. 1848–1859 (1981).
 25. Kulkarni, A. K., Jacob, H. R. and Hwang, J. J., "Similarity Solution for Natural Convection Flow over an Isothermal Vertical Wall Immersed in a Thermally Stratified Medium," *International Journal Heat and Mass Transfer*, **30**, pp. 691–698 (1987).
 26. Angirasa, D. and Srinivasan, J., "Natural Convection Flows Due to the Combined Buoyancy of Heat and Mass Transfer in a Thermally Stratified Medium," *Journal of Heat Transfer*, ASME, **111**, pp. 657–663 (1989).
 27. Takhar, H. S., Chamkha, A. J. and Nath, G., "Natural Convection Flow from a Continuously Moving Vertical Surface Immersed in a Thermally Stratified Medium," *Heat and Mass Transfer*, **38**, pp. 17–24 (2001).
 28. Ishak, A., Nazar, R. and Pop, I., "Mixed Convection Boundary Layer Flow Adjacent to a Vertical Surface Embedded in a Stable Stratified Medium," *International Journal Heat and Mass Transfer*, **51**, pp. 3693–3695 (2008).
 29. Bejan, A., *Convection Heat Transfer*, John Wiley & Sons, New York (1984).
 30. Chang, C.-L. and Lee, Z.-Y., "Free Convection on a Vertical Plate with Uniform and Constant Heat Flux in a Thermally Stratified Micropolar Fluid," *Mechanics Research Communications*, **35**, pp. 421–427 (2008).
 31. Perdakis, C. and Raptis, A., "Heat Transfer of a Micropolar Fluid by the Presence of Radiation," *Heat and Mass Transfer*, **31**, pp. 381–382 (1996).
 32. Kim, Y. I. and Fedorov, A. G., "Transient Mixed Radiation Convection Flow of a Micropolar Fluid Past a Moving, Semi-Infinite Vertical Porous Plate," *International Journal Heat and Mass Transfer*, **46**, pp. 1751–1758 (2003).
 33. Raptis, A., "Flow of a Micropolar Fluid Past a Continuously Moving Plate by the Presence of Radiation," *International Journal Heat and Mass Transfer*, **41**, pp. 2865–2866 (1998).
 34. Mahmoud, M. A. A., Mahmoud, A. E. M., Waheed, S. E., "Hydromagnetic Boundary Layer Micropolar Fluid Flow over a Stretching Surface Embedded in a Non-Darcian Porous Medium in the Presence of Radiation," *Mathematical Problems in Engineering*, pp. 1–10 (2006).
 35. Raptis, A., "Radiation and Free Convection Flow Through a Porous Medium," *International Communications Heat and Mass Transfer*, **25**, pp. 289–295

- (1998).
36. Ahmadi, G., "Self-Similar Solution of Incompressible Micropolar Boundary Layer Flow over a Semi-Infinite Plate," *International Journal of Engineering Science*, **14**, pp. 639–646 (1976).
 37. Kline, K. A., "A Spin Vorticity Relation for Unidirectional Plane Flows of Micropolar Fluids," *International Journal of Engineering Science*, **15**, pp. 131–134 (1977).
 38. Jena, S. K. and Mathur, M. N., "Similarity Solution for Laminar Free Convection Flow of Thermo-Micropolar Fluid Past a Non-Isothermal Vertical Flat Plate," *International Journal of Engineering Science*, **19**, pp. 1431–1439 (1981).
 39. Peddieson, J. and McNitt, R. P., "Boundary Layer Theory for a Micropolar Fluid," *Recent Advances in Engineering Science*, **5**, pp. 405–426 (1970).
 40. Raptis, A., "Radiation and viscoelastic flow," *International Communications Heat and Mass Transfer*, **26**, pp. 889–895 (1999).
 41. El-Gendi, S. E., "Chebyshev Solution of Differential, Integral and Integro-Differential Equations," *Computer Journal*, **12**, pp. 282–287 (1969).
 42. Morchoisne, Y., "Pseudo-Spectral Space-Time Calculations of Incompressible Viscous Flows," *AIAA Journal*, **19**, pp. 81–82 (1981).
 43. Ishak, A., Nazar, R. and Pop, I., "Hydromagnetic Flow and Heat Transfer Adjacent to a Stretching Vertical Sheet," *Heat and Mass Transfer*, **44**, pp. 921–927 (2008).
 44. Ali, F. M., Nazar, R., Arifin, N. M. and Pop, I., "Effect of Hall Current on MHD Mixed Convection Boundary Layer Flow over a Stretched Vertical Flat Plate," *Meccanica*, **46**, pp. 1103–1112 (2011).
 45. Prandtl, L., *Essentials of Fluid Dynamics*, Blackie, London (1952).
 46. Jaluria, Y. and Himasekhar, K., "Buoyancy Induced Two Dimensional Vertical Flows in a Thermally Stratified Environment," *Computer and Fluids*, **11**, pp. 39–49 (1983).

(Manuscript received May 16, 2012,
accepted for publication December 17, 2012.)